Selective Adsorption of Glucose towards Itaconic Acid on Amorphous Silica Surfaces: Insights from Density Functional Theory Calculations

Saber Gueddida, Michael Badawi, Hilda Elizabeth Reynel-Ávila, Adrián Bonilla-Petriciolet, Sébastien Lebègue

Version of Record: https://www.sciencedirect.com/science/article/pii/S0167732221023114
Manuscript_8b8a0fe6a082c6932a5cac9cd84866f1

Selective Adsorption of Glucose towards Itaconic Acid on Amorphous Silica Surfaces: insights from density functional theory calculations

Saber Gueddida[a,*], Michael Badawi[a,*], Hilda Elizabeth Reynel-Ávila[b,c,*], Adrián Bonilla-Petriciolet[b,*], Sébastien Lebègue[a,*]

[a] *Lorraine University, Laboratoire de Physique et Chimie Théoriques, CNRS:UMR-7019, Vandoeuvre-lès-Nancy 54506, France.*
[b] *Instituto Tecnológico de Aguascalientes, Aguascalientes, 20256, Mexico.*
[c] *CONACyT, Cátedras jóvenes investigadores, Ciudad de Mexico, 03940, Mexico.*

Abstract

A better separation and purification of organic acids in liquid phase is a key for a more performing biorefinery industry. Herein, amorphous silica surfaces with a density of silanol ranging between 1.1 and 7.2 OH·nm^{-2} are investigated to separate glucose molecules from the fermentation broths. Different interaction modes of glucose and itaconic acid on the considered silica surfaces at various silanol sites are systematically investigated using periodic density functional theory. Our results show that the surfaces with a silanol density of 2.0 to 7.2 OH·nm^{-2} are potentially selective for glucose adsorption in comparison with itaconic acid.

Keywords: DFT, Selective Adsorption, Organic Acids, Amorphous silica surfaces.

1. Introduction

Recently, the production of bio-based compounds from renewable biomasses via biological or chemical conversion has increased its relevance and commercial importance to substitute the chemicals and products obtained from petrochemical industry [1, 2, 3, 4, 5]. In 2004, the report Top Value Added Chemicals from Biomass of U.S. Department of Energy identified twelve building block chemicals promising for industry, which are sugar-based molecules useful to obtain a wide spectrum of high-value bio-based products. In this direction, the production of organic acids via biomass fermentation has emerged as a fast-evolving and competitive industrial alternative. These organic acids are commodity chemicals that can

* *Email addresses:* saber.gueddida@univ-lorraine.fr (Saber Gueddida), michael.badawi@univ-lorraine.fr (Michael Badawi), hereynelav@conacyt.mx (Hilda Elizabeth Reynel-Ávila), petriciolet@hotmail.com (Adrián Bonilla-Petriciolet), sebastien.lebegue@univ-lorraine.fr (Sébastien Lebègue)

be employed, for example, as polymer building blocks since they are considered sustainable, cost-effective and environmentally friendly [1, 3, 5, 6, 7].

In particular, the itaconic acid is one of the twelve building blocks with a significant industrial potential. This compound is an unsaturated organic diacid with two carboxylic groups [8]. It can be employed as an efficient intermediate for several reactions such as anhydride formation, salt formation with metals, polymerization, esterification and others [3]. This acid is used to produce unsaturated polyester resins, synthetic latex, styrene-butadiene rubber latex, chelant dispersant agents, methyl methacrylate, superabsorbent polymers, glass, oil additives and phosphate-free detergents besides other applications in the industrial sectors of food, agriculture, health and pharmacy [9, 3]. USA, China and India are the main producers of itaconic acid generating around 41,000 tons/year [10, 3].

The production of this organic acid relies mainly on the aerobic fungal fermentation with Aspergillus terreus and starts with a glucose source [3]. The itaconic acid must be separated from the final fermentation broth in order to enhance its quality. Therefore, the recovery and purification of this acid is a key step for its industrial production. Crystallization is the classical method for itaconic acid recovery, which consists basically of evaporation and cooling of the solution thus obtaining global yields of 51 - 80% where the crystallization performance is affected by the residual glucose [9, 11, 12]. Herein, it is convenient to highlight that the production and commercialization of this organic acid from fermentation process is limited due to the product recovery from diluted broths is a cost intensive process [10]. Some models indicated that the recovery and purification can represent 30 - 40% of the final product costs [12, 13]. Therefore, the low-cost production of high-quality itaconic acid relies significantly on its successful purification and recovery where a low energy consumption is desirable from both technical, economic and environmental points of view. The development of effective and low-cost technologies for itaconic acid recovery is a necessity to compete with the petroleum-based compounds.

To date, other alternatives to crystallization have been tested and analyzed for itaconic acid recovery including precipitation, reactive extraction, electrodialysis, membrane separation and adsorption [3, 8, 10]. Adsorption has emerged as a straightforward, cost-effective and environmentally friendly method to recover this organic acid from fermentation broths. Previous studies have demonstrated the potential of this purification process [8, 13, 14]. For instance, Magalahes et al. [8] reported the itaconic acid separation using PFA-300 and Purolite A-500P ion-exchange resins. Batch experiments were performed to analyze the effect of temperature, initial itaconic acid concentration and pH. Fixed-bed column tests were also carried out to calculate design parameters with a simplified model. The resin PFA-300 was more effective for itaconic acid recovery with a maximum adsorption capacity of 0.154 $g_{IA} \cdot g_{resin}^{-1}$. Schute et al. [14] studied the itaconic acid separation from binary (itaconic acid + glucose) solutions as well as fermentation broths using highly hydrophobic adsorbents such as hyper-cross-linked polymers, zeolites and activated carbons. The adsorbents with highly hydrophobic nature showed the highest selectivity in batch and continuous adsorbers

[14]. The molar ratios of glucose over itaconic acid in the fermentation broths can vary from 0.26 to 3.5 depending on the operating conditions [15, 16]. As this range is relatively small we do not expect a particular influence of the glucose/itaconic acid molar ratio on the adsorption selectivity performance. Magalhaes et al. [17] simulated the itaconic acid recovery with electrodialysis, reactive extraction and adsorption to compare their performance and productions costs for different downstream trains. These simulations showed that the adsorption had a significant potential as alternative to crystallization showing very similar process performances.This study also concluded that electrodialysis was the worst option for this separation.

It is clear that the tailoring of adsorbent properties is fundamental to improve the itaconic acid recovery and, consequently, for reducing the operating costs. Based on this fact, this paper reports the theoretical analysis of the adsorption and selectivity of itaconic acid recovery on silica surfaces via periodic density functional theory (DFT) calculations. Among the available supports, silica-based materials (zeolites and silica), titania and alumina are the most used today due to their abundance, low cost and also physico-chemical properties [18, 19, 20, 21]. Most of them are amorphous due to their high porosity and superior performance compared to the crystalline structures [22]. Amorphous silica surface is a relevant support for diverse applications because of its chemical modification selectivity, high dielectric strength and mechanical resistance [23, 24, 25, 26, 27]. Therefore, this study analyzes the interactions of itaconic acid and glucose, which are the main components of fermentation broths to produce this organic acid, with amorphous silica surfaces having various densities of silanol. It has been shown in the past that DFT calculations allowed to identify efficient formulations of adsorbents in various selective trapping applications like the purification of biofuels via the separation of toluene and phenol [28, 29, 30, 31] and the removal of iodine species released during nuclear accidents [32, 33, 34]. These results are useful to estimate and characterize the performance of this potential adsorbent for the recovery and purification of this organic acid.

2. Method of calculations

Periodic Density Functional Theory (DFT) calculations have been realized using the PBE+D2 method [35, 36] as implemented in the Vienna Ab Initio Simulation Package (VASP) [37]. The projector-augmented wave (PAW) approach has been used [38, 39] and the cutoff energy set to 450 eV. Due to the large size of the supercell, we used only the Γ point to sample the first Brillouin zone. The convergence criterion for the electronic self-consistent loop for the difference in total energy is fixed to 10^{-6}eV. Because the aim is to elucidate the adsorption mechanism of a single molecule on amorphous surfaces, the positions of the title molecules and the top layer of the substrate (O, H, and Si atoms) are relaxed, while the bottom layers were kept frozen. The force criterion for relaxation was fixed to 0.03 eV/Å.

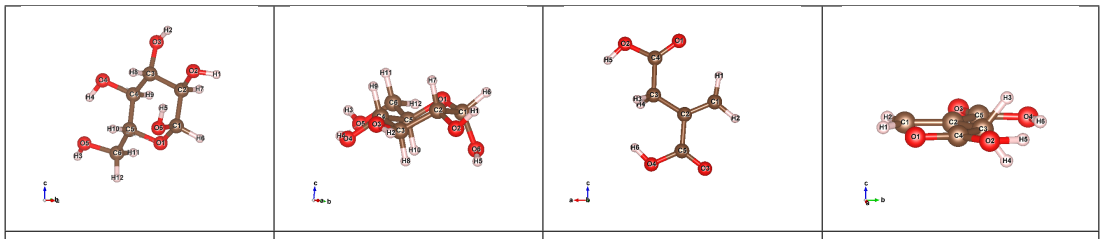

(a) Glucose: $O^{\perp}$ int (b) Glucose: $O^{\parallel}$ int (c) Itaconic acid: $O^{\perp}$ int (d) Itaconic acid: $O^{\parallel}$ int

Figure 1: Top and side views of the molecular structures of glucose and itaconic acid, which correspond to $O^{\perp}$ and $O^{\parallel}$ int modes, respectively.

3. Results and discussions

3.1. Structural models

In this work, we have studied the interaction between the glucose or the itaconic acid molecule and the silica surfaces with a density of silanol equal to 7.2, 5.9, 4.6, 3.3, 2.0, and 1.1 OH·nm^{-2}, respectively (denoted silica-7.2, silica-5.9, silica-4.6, silica-3.3, silica-2.0 and silica-1.1). These surfaces were modeled by A. Comas Vives [40] via dehydroxylation of an entire hydroxylated surface with a super cell of 402 atoms for silica-7.2, 393 atoms for silica-5.9, 384 atoms for silica-4.6, 375 atoms for silica-3.3, 376 atoms for silica-2.0 and 372 atoms for silica-1.1 [31, 40, 41, 42, 43]. The surfaces having a density of silanol ranging between 3.3 and 7.2 OH·nm^{-2} contain all silanol groups (nest-1, nest-2, isolated, geminal, and vicinal). The silica-2.0 contains the nest-1, vicinal, and isolated silanol groups, while silica-1.1 displays only the isolated ones [31, 41, 42, 40]. The glucose molecule contains 24 atoms; 6 carbon, 6 oxygen and 12 hydrogen atoms, while the itaconic acid molecule is composed of 5 carbon, 4 oxygen and 6 hydrogen atoms. The lattice parameters of all the considered systems are a = 21.39Å, b = 21.39Å, c = 34.17Å, α=90°, β=90° and γ=90°. A vacuum of 20 Å was used in the z direction to separate the periodically repeated cells.

Several structural configurations were calculated to identify the most favorable adsorption configurations of glucose and itaconic acid molecule onto different surfaces with various densities of silanol. The calculations were firstly started from two interaction modes (see Figure 1) at various silanol sites on surfaces: the perpendicular O interaction ($O^{\perp}$ int) through one or two oxygen atoms, and the flat O interaction ($O^{\parallel}$ int) through at least two oxygen atoms but it is possible that all the oxygen atoms are contributing. For both interaction modes, we considered all the possible orientations of the molecule at each adsorption position (possible silanol groups).

3.2. Adsorption properties

For both interaction modes, the calculated adsorption energies of the title compounds on various silanol density surfaces at different silanol sites are summarized in Table 1. The adsorption energies ΔE_{ads} are given by:

$$\Delta E_{ads} = E_{TotSys} - E_{Mol} - E_{Surf}, \quad (1)$$

Table 1: Computed adsorption energy (in kJ·mol^{-1}) of glucose and itaconic acid on surfaces for each adsorption mode using the PBE+D2 approximation.

Surface	Molecule	O int mode	Isolated	Nest-1	Vicinal	Nest-2	Geminal
silica-1.1	Glucose	$O^{\perp}$ int	-74				
		$O^{\parallel}$ int	-59				
	Itaconic-Acid	$O^{\perp}$ int	-32				
		$O^{\parallel}$ int	-72				
silica-2.0	Glucose	$O^{\perp}$ int	-76	-108	-61		
		$O^{\parallel}$ int	-67	-115	-62		
	Itaconic-Acid	$O^{\perp}$ int	-30	-24	-1		
		$O^{\parallel}$ int	-61	-71	-49		
silica-3.3	Glucose	$O^{\perp}$ int	-76	-114	-93	-108	-81
		$O^{\parallel}$ int	-71	-112	-88	-68	-93
	Itaconic-Acid	$O^{\perp}$ int	-33	-45	-48	-40	-34
		$O^{\parallel}$ int	-79	-84	-102	-89	-62
silica-4.6	Glucose	$O^{\perp}$ int	-79	-141	-135	-103	-89
		$O^{\parallel}$ int	-57	-150	-144	-77	-97
	Itaconic-Acid	$O^{\perp}$ int	-3	-67	-44	-41	-32
		$O^{\parallel}$ int	-83	-131	-108	-62	-104
silica-5.9	Glucose	$O^{\perp}$ int	-47	-127	-110	-125	-107
		$O^{\parallel}$ int	-77	-149	-125	-143	-84
	Itaconic-Acid	$O^{\perp}$ int	-2	-62	-44	-59	-47
		$O^{\parallel}$ int	-69	-105	-115	-109	-105
silica-7.2	Glucose	$O^{\perp}$ int	-64	-150	-139	-138	-104
		$O^{\parallel}$ int	-93	-198	-160	-151	-141
	Itaconic-Acid	$O^{\perp}$ int	-32	-49	-56	-68	-52
		$O^{\parallel}$ int	-120	-125	-130	-157	-94

where E_{TotSys}, E_{Surf} and E_{Mol} are the PBE+D2 total energy of glucose@silica or itaconic-Acid@silica system, the isolated surface and the isolated glucose or itaconic-acid molecule, respectively.

The silica-1.1 surface presents only the isolated sites; the most stable configurations for glucose and itaconic acid are, respectively, $O^{\perp}$ and $O^{\parallel}$ interaction modes with ΔE_{ads} of -74 kJ·mol^{-1} and -72 kJ·mol^{-1}. The two molecules exhibit similar inetraction energies on this surface. However, the adsorption energy of glucose on the silica-2.0 surface on the nest-1 site

Table 2: Calculated adsorption energy (in kJ·mol^{-1}) of the most stable configuration of glucose, itaconic acid and water on surfaces with different densities of silanol using the PBE+D2 approximation.

	silica-1.1	silica-2.0	silica-3.3	silica-4.6	silica-5.9	silica-7.2
Glucose	-74	-115	-114	-150	-149	-198
Itaconic-Acid	-72	-71	-102	-131	-115	-157
Water [31]	-33	-55	-70	-81	-76	-85

via a $O^{\parallel}$ interaction mode is 44 kJ·mol^{-1} larger than that of itaconic acid. Our results show a significant adsorption energy of -108 kJ·mol^{-1} for the glucose molecule also on the same site but via a $O^{\perp}$ interaction mode. The most stable configuration for glucose and itaconic acid adsorption on silica-3.3 is a $O^{\perp}$ int on the nest-1 with ΔE_{ads} of -114 kJ·mol^{-1}, while for itaconic acid is a $O^{\parallel}$ int on the vicinal silanol group with -102 kJ·mol^{-1}. A larger energy value is observed also for the glucose molecule on the vicinal and nest-2 silanol groups. For silica-4.6 surface, both molecules prefer to occupy the silanol group nest-1 through a $O^{\parallel}$ int mode with ΔE_{ads} equal to -150 kJ·mol^{-1} for glucose and -131 kJ·mol^{-1} for the itaconic acid. Our calculations show also that glucose is strongly connected to the nest-1 via a $O^{\perp}$ int mode (-114 kJ·mol^{-1}), the vicinal via both $O^{\parallel}$ (-144 kJ·mol^{-1}) and $O^{\perp}$ (-135 kJ·mol^{-1}) int and the nest-2 via a $O^{\perp}$ interaction (-103 kJ·mol^{-1}), while the itaconic acid prefers to accommodate on the vicinal and the geminal adsorption sites via a $O^{\parallel}$ int mode with ΔE_{ads} equal to -108 and -104 kJ·mol^{-1}, respectively. The larger interaction energies for the glucose and the itaconic acid molecules on silica-5.9 surface are found on the nest-1 and 2 silanol groups, respectively, via a $O^{\parallel}$ interaction with ΔE_{ads} of -149 and -109 kJ·mol^{-1}. Both molecules are strongly adsorbed on the nest-1, nest-2, vicinal, and geminal sites via the two O int modes for glucose and a $O^{\parallel}$ int mode for itaconic acid. For the silica-7.2 surface, glucose always prefers to acommodate on the silanol group nest-1 through a $O^{\parallel}$ interaction with a high value of -198 kJ·mol^{-1}, while the itaconic acid is connected to the nest-2 with an adsorption energy of -157 kJ·mol^{-1}. We found that the two molecules exhibit significant adsorption energies on all the silanol adsorption groups through both O int modes for glucose and a $O^{\parallel}$ int mode for itaconic acid. Our calculations show that the most favorable configuration for both glucose and itaconic acid adsorption are a $O^{\parallel}$ int mode, where the interaction through the oxygen atoms are maximized.

3.3. The most stable adsorption structures

Table 2 shows the PBE+D2 adsorption energies of glucose and itaconic acid corresponding to their most favorable structures on silica-1.1, silica-2.0, silica-3.3, silica-4.6, silica-5.9, and silica-7.2 surfaces. The resulting adsorption energies show that all the considered surfaces with various densities of silanol promote the adsorption of the glucose molecule compared to the itaconic acid, except for the silica-1.1 surface where both molecules exhibit similar adsorption energies, which is mainly due to the number of established OH bonds.

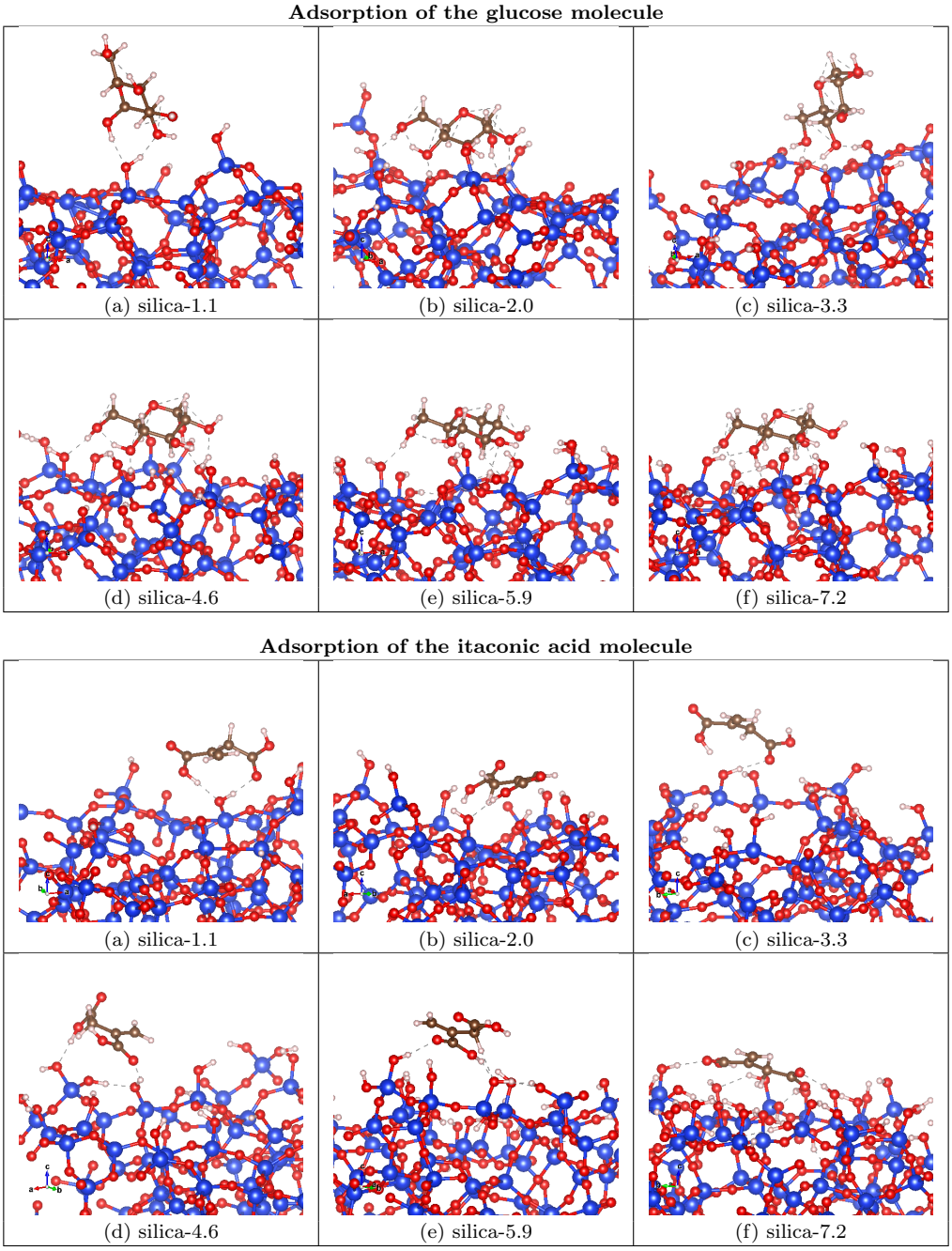

Figure 2: The most stable geometry interaction of (first panels) the glucose and of (second panels) the itaconic acid molecules on (a) silica-1.1, (b) silica-2.0, (c) silica-3.3, (d) silica-4.6, (e) silica-5.9, and (f) silica-7.2 surfaces.

Our calculations show that the adsorption energies of glucose on silica-2.0, silica-3.3, silica-4.6, silica-5.9, and silica-7.2 surface are 44, 12, 19, 34, and 41 kJ·mol^{-1} larger than those of the itaconic acid. This makes the surfaces with a density of silanol ranging between 2.0 and 7.2 OH·nm^{-2} potentially selective toward glucose adsorption. A large interaction energy

for the glucose and the itaconic acid is observed on the silica-7.2 surface with ΔE_{ads} equal, respectively, to -198 and 157 kJ·mol^{-1}. In addition, we found that the adsorption energy of both molecules increases with the silanol density surface. For the highest density of silanol, the silanol groups would be close enough to establish other interactions between the oxygen of the molecule and the silanol OH groups. For water, the adsorption energies of the most stable configurations on silica-1.1, silica-2.0, silica-3.3, silica-4.6, silica-5.9, and silica-7.2 are found to be -33, -55, -81, -76, and -85 kJ·mol^{-1}, respectively (see Table 2 and more details are given in [31]). For all cases, our results show that the water molecule is in general less adsorbed than the glucose and itaconic acid ones. The inhibiting effect of water on the adsorption of glucose and itaconic acid is therefore expected to be negligible over all silica surfaces.

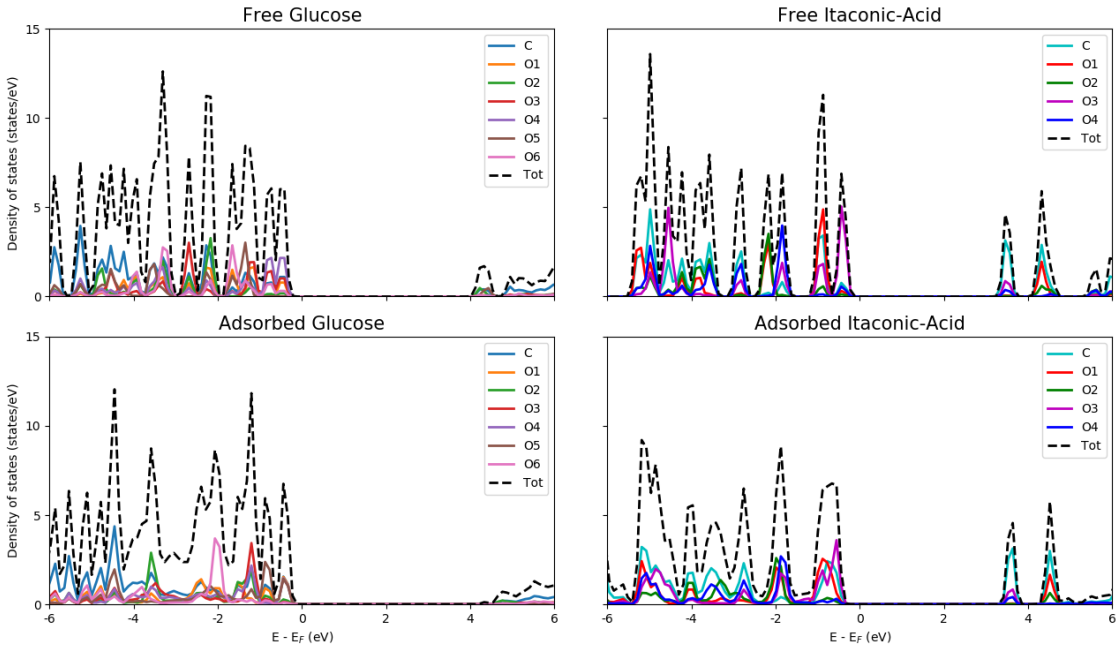

Figure 3: Total and projected density of states for the isolated and the most stable interacted glucose and itaconic acid molecules on silica-7.2 surface via O$^{\|}$ int mode at nest-1 and nest-2 silanol sites, respectively.

The most stable interaction structures for the glucose and the itaconic acid on various surfaces are shown in Figure 2. In all cases, the interaction between the considered molecules and the silica surfaces is established by the formation of OH bonds between the oxygen atom of the molecule and the hydrogen atom of the silanol group or between the hydrogen atom of the molecule and the oxygen atom of the silanol surface group. Our results show the creation of two OH bonds, when the title compounds are adsorbed on the silica-1.1 surface with distance values of 1.67 and 1.83 Å for glucose and 1.70 and 1.68 Å for itaconic acid. For the silica-2.0 surface, four OH bonds are established between the glucose molecule and the silica surface with distance values of 1.73, 1.87, 1.69, and 1.79 Å, and one OH bond of 1.84 Å for the itaconic acid. Four OH bonds created between the glucose and the silanol groups of silica-3.3 with distance values in the range of 1.51-1.78 Å and only one hydrogen bond

of 1.86 Å. Also, four hydrogen bonds are established between the glucose and the silica-4.6 surface (1.76-1.88 Å) and two OH bonds for the itaconic acid with distance values of 1.72 and 1.82 Å. For the silica-5.9 surface, our results show the formation of five OH bonds for the glucose molecule and two OH bonds for the itaconic acid with distance values in the range of 1.68-1.98 Å and 1.70-1.89 Å, respectively. For the silica-7.2 surface, the glucose and the itaconic acid molecules are strongly adsorbed onto the silica surface through six OH bonds of 1.73-1.86 Å and three OH bonds of 1.74-1.95 Å, respectively. We have also observed that the geometrical structure of the considered molecules influenced by the surface, in particular for the itaconic acid on silica-4.6, where the symmetry of the molecule is broken.

Figure 3 shows the total and the projected density of states of the isolated and the most stable adsorbed glucose and itaconic acid molecules on silica-7.2 surface. By comparing the total density of states of the adsorbed and the isolated molecule, we found a broadening of the different peaks when the molecule is adsorbed onto silica surface. This broadening is due to the strong hybridization between the molecular and the surface levels. In addition, for the itaconic acid molecule, we found a slight shift of all peaks to lower and higher energies, respectively, which result in an increase of the band gap from 3.91 eV for the free molecule to 4.08 eV for the adsorbed one. However, for the glucose molecule, both occupied and unoccupied peaks are slightly displaced to the Fermi level, and therefore, a small reduction of the band gap from 4.71 eV to 4.38 eV due to the silica surface is observed.

4. Conclusions

In this work, using density functional theory calculations, we showed the potential of amorphous silica surfaces with different density of silanol ranging between 1.1 and 7.2 $OH{\cdot}nm^{-2}$ for the selective adsorption of the glucose molecule versus itaconic acid. We have investigated systematically several geometrical configurations of the title compounds on various surfaces at different locations and adsorption modes (perpendicular or flat O interaction). The resulting adsorption energies show that all the considered surfaces with various densities of silanol favor the adsorption of glucose rather than itaconic acid, except for silica-1.1 surface where the adsorption energies of the two molecules are similar. We found that the adsorption energy of glucose and itaconic acid molecules increases with the silanol density surface. This makes the surfaces with a density of silanol ranging between 2.0 and 7.2 $OH{\cdot}nm^{-2}$ potentially very selective towards glucose adsorption. Our finding suggest that silica materials could be used as purification membranes for the recovery of itaconic acid from the final fermentation broths in the biomass-based industry.

Acknowledgements

This work was performed using the Lorraine University HPC Mesocenter "Explor" and TGCC under the allocation 2021-A0100810433 by GENCI-EDARI. SG, MB and SB also acknowledge financial support through the COMETE project (COnception in silico de Matériaux pour l'EnvironmenT et l'Energie) cofunded by the European Union under the program "FEDER-FSE Lorraine et Massif des Vosges 2014-2020".

References

[1] J. Becker, A. Lange, J. Fabarius, C. Wittmann, Top value platform chemicals: bio-based production of organic acids, Curr. Opin. Biotechnol. 36 (2015) 168–175. doi:10.1016/j.copbio.2015.08.022.

[2] J. Serafin, M. Baca, M. Biegun, E. Mijowska, R. J. Kalenczuk, J. Srenscek-Nazzal, B. Michalkiewicz, Direct conversion of biomass to nanoporous activated biocarbons for high CO2 adsorption and supercapacitor applications, Appl. Surf. Sci. 497 (2019) 143722. doi:10.1016/j.apsusc.2019.143722.

[3] B.-E. Teleky, D. C. Vodnar, Biomass-Derived Production of Itaconic Acid as a Building Block in Specialty Polymers, Polymers 11. doi:10.3390/polym11061035.

[4] J. Li, M. Zahid, W. Sun, X. Tian, Y. Zhu, Synthesis of Pt supported on mesoporous g-C3N4 modified by ammonium chloride and its efficiently selective hydrogenation of furfural to furfuryl alcohol, Appl. Surf. Sci. 528 (2020) 146983. doi:10.1016/j.apsusc.2020.146983.

[5] Y. Zhai, M. Chu, N. Shang, C. Wang, H. Wang, Y. Gao, Bimetal Co8Ni2 catalyst supported on chitin-derived N-containing carbon for upgrade of biofuels, Appl. Surf. Sci. 506 (2020) 144681. doi:10.1016/j.apsusc.2019.144681.

[6] F. Ma, L. He, E. Lindner, D.-Y. Wu, Highly porous poly(l-lactic) acid nanofibers as a dual-signal paper-based bioassay platform for in vitro diagnostics, Appl. Surf. Sci. 542 (2021) 148732. doi:10.1016/j.apsusc.2020.148732.

[7] M. Masoumi, M. Jahanshahi, M. G. Ahangari, G. N. Darzi, Electronic, mechanical and thermal properties of SiO2 nanotube interacting with poly lactic-co-glycolic acid: Density functional theory and molecular dynamics studies, Appl. Surf. Sci. 546 (2021) 148894. doi:10.1016/j.apsusc.2020.148894.

[8] A. I. Magalhaes, J. C. de Carvalho, E. N. M. Ramirez, J. D. C. Medina, C. R. Soccol, Separation of Itaconic Acid from Aqueous Solution onto Ion-Exchange Resins, J. Chem. Eng. Data 61 (2016) 430–437. doi:10.1021/acs.jced.5b00620.

[9] M. Okabe, D. Lies, S. Kanamasa, E. Y. Park, Biotechnological production of itaconic acid and its biosynthesis in aspergillus terreus, Apll. Microbiol. Biotechnol. 84 (2009) 597–606. doi:10.1007/s00253-009-2132-3.

[10] R. Bafana, R. A. Pandey, New approaches for itaconic acid production: bottlenecks and possible remedies, Crit. Rev. Biotechnol. 38 (1) (2018) 68–82. doi:10.1080/07388551.2017.1312268.

[11] N. J. Vickers, Animal communication: When im calling you, will you answer too?, Curr. Biol. 27 (2017) R713–R715. doi:10.1016/j.cub.2017.05.064.

[12] S. Li, Z. Jiang, W. Xu, Y. Xie, L. Zhao, X. Tang, F. Wang, F. Xin, Stachybotrys chlorohalonata, suppresses proliferation and migration in lung cancer cells, Appl. Microbiol. Biotechnol. 101 (2017) 3227–3235. doi:10.1007/s00253-016-8030-6.

[13] H. De Wever, D. Dennewald, Screening of sorbents for recovery of succinic and itaconic acid from fermentation broths, J. Chem. Technol. Biotechnol. 93 (2) (2018) 385–391. doi:10.1002/jctb.5366.

[14] K. Schute, C. Detoni, A. Kann, O. Jung, R. Palkovits, M. Rose, Separation in Biorefineries by Liquid Phase Adsorption: Itaconic Acid as Case Study, ACS Sustain. Chem. Eng. 4 (2016) 5921–5928. doi:10.1021/acssuschemeng.6b00096.

[15] J. Gorden, E. Ceiser, N. Wierckx, L. M. Blank, T. Zeiner, C. Brandenbusch, Integrated process development of a reactive extraction concept for itaconic acid and application to a real fermentation broth, Eng. Life Sci. 17 (2017) 809–816. doi:10.1002/elsc.201600253.

[16] A. Heverkerl, A. Kuenz, K.-D. Vorlop, Influence of the ph on the itaconic acid production with aspergillus terreus, Applied Microbiology and Biotechnology 98 (2014) 10005–10012.

[17] A. I. Magalhaes, J. C. de Carvalho, J. F. Thoms, J. D. C. Medina, C. R. Soccol, Techno-economic analysis of downstream processes in itaconic acid production from fermentation broth, J. Clean. Prod. 206 (2019) 336–348. doi:10.1016/j.jclepro.2018.09.204.

[18] C. Chizallet, P. Raybaud, Density functional theory simulations of complex catalytic materials in reactive environments: beyond the ideal surface at low coverage, Catal. Sci. Technol. 4 (2014) 2797–2813. doi:10.1039/C3CY00965C.

[19] S. Simonetti, A. D. Company, E. Pronsato, A. Juan, G. Brizuela, A. Lam, Density functional theory

based-study of 5-fluorouracil adsorption on β-cristobalite(111) hydroxylated surface: The importance of H-bonding interactions, Appl. Surf. Sci. 359 (2015) 474–479. doi:10.1016/j.apsusc.2015.10.147.

[20] A. B. Schvval, A. Juan, G. F. Cabeza, Theoretical study of the role of the interface of Ag_4 nanoclusters deposited on TiO_2(110) and TiO_2(101), Appl. Surf. Sci. 490 (2019) 343–351. doi:10.1016/j.apsusc.2019.05.291.

[21] I. Graca, J. Lopes, M. Ribeiro, M. Badawi, S. Laforge, P. Magnoux, F. Ramoa Ribeiro, n-heptane cracking over mixtures of hy and hzsm-5 zeolites: Influence of the presence of phenol, Fuel 94 (2012) 571–577. doi:10.1016/j.fuel.2011.11.033.

[22] B. R. Goldsmith, B. Peters, J. K. Johnson, B. C. Gates, S. L. Scott, Beyond Ordered Materials: Understanding Catalytic Sites on Amorphous Solids, ACS Catal. 7 (2017) 7543–7557. doi:10.1021/acscatal.7b01767.

[23] H. Guesmi, R. Gryboś, J. Handzlik, F. Tielens, Characterization of molybdenum monomeric oxide species supported on hydroxylated silica: a DFT study, Phys. Chem. Chem. Phys. 16 (2014) 18253–18260. doi:10.1039/C4CP02296C.

[24] M. Gierada, P. Michorczyk, F. Tielens, J. Handzlik, Reduction of chromia-silica catalysts: A molecular picture, J. Catal. 340 (2016) 122–135. doi:10.1016/j.jcat.2016.04.022.

[25] B. R. Goldsmith, B. Peters, J. K. Johnson, B. C. Gates, S. L. Scott, Beyond Ordered Materials: Understanding Catalytic Sites on Amorphous Solids, ACS Catal. 7 (2017) 7543–7557. doi:10.1021/acscatal.7b01767.

[26] T. Siodla, I. Sobczak, M. Ziolek, F. Tielens, Theoretical and experimental insight into zinc loading on mesoporous silica, Micropor. Mesopor. Mat. 256 (2018) 199–205. doi:10.1016/j.micromeso.2017.08.008.

[27] F. Tielens, M. Gierada, J. Handzlik, M. Calatayud, Characterization of amorphous silica based catalysts using DFT computational methods, Catal. Today 354 (2020) 3–18. doi:10.1016/j.cattod.2019.03.062.

[28] I. Khalil, H. Jabraoui, G. Maurin, S. Lebegue, M. Badawi, K. Thomas, F. Mauge, Selective Capture of Phenol from Biofuel Using Protonated Faujasite Zeolites with Different Si/Al Ratios, J. Phys. Chem. C 122 (2018) 26419–26429. doi:10.1021/acs.jpcc.8b07875.

[29] H. Jabraoui, I. Khalil, S. Lebegue, M. Badawi, Ab initio screening of cation-exchanged zeolites for biofuel purification, Mol. Syst. Des. Eng. 4 (2019) 882–892. doi:10.1039/C9ME00015A.

[30] I. Khalil, H. Jabraoui, S. Lebegue, W. J. Kim, L.-J. Aguilera, K. Thomas, F. Mauge, M. Badawi, Biofuel purification: Coupling experimental and theoretical investigations for efficient separation of phenol from aromatics by zeolites, Chem. Eng. Technol. 402 (2020) 126264. doi:10.1016/j.cej.2020.126264.

[31] S. Gueddida, S. Lebegue, M. Badawi, Assessing the Potential of Amorphous Silica Surfaces for the Removal of Phenol from Biofuel: A Density Functional Theory Investigation, J. Phys. Chem. C 124 (2020) 20262–20269. doi:10.1021/acs.jpcc.0c06581.

[32] S. Chibani, I. Medlej, S. Lebegue, J. G. Angyan, L. Cantrel, M. Badawi, Performance of CuII-, PbII-, and HgII-Exchanged Mordenite in the Adsorption of I2, ICH3, H2O, CO, ClCH3, and Cl2: A Density Functional Study, Chem. Phys. Chem. 18 (2017) 1642–1652. doi:10.1002/cphc.201700104.

[33] H. Jabraoui, E. Hessou, S. Chibani, L. Cantrel, S. Lebegue, M. Badawi, Adsorption of volatile organic and iodine compounds over silver-exchanged mordenites: A comparative periodic DFT study for several silver loadings, Appl. Surf. Sci. 485 (2019) 56–63. doi:10.1016/j.apsusc.2019.03.282.

[34] M. Chebbi, S. Chibani, J.-F. Paul, L. Cantrel, M. Badawi, Evaluation of volatile iodine trapping in presence of contaminants: A periodic DFT study on cation exchanged-faujasite, Micropor. Mesopor. Mat. 239 (2017) 111–122. doi:10.1016/j.micromeso.2016.09.047.

[35] J. P. Perdew, K. Burke, M. Ernzerhof, Generalized Gradient Approximation Made Simple, Phys. Rev. Lett. 77 (1996) 3865–3868. doi:10.1103/PhysRevLett.77.3865.

[36] S. Grimme, Semiempirical GGA-type density functional constructed with a long-range dispersion correction, J. Comput. Chem. 27 (15) (2006) 1787–1799. doi:10.1002/jcc.20495.

[37] T. Bucko, J. Hafner, S. Lebègue, J. G. Angyán, Improved Description of the Structure of Molecular and Layered Crystals: Ab Initio DFT Calculations with van der Waals Corrections, J. Phys. Chem. A 114 (43) (2010) 11814–11824. doi:10.1021/jp106469x.

[38] P. E. Blöchl, Projector augmented-wave method, Phys. Rev. B 50 (1994) 17953–17979.

doi:10.1103/PhysRevB.50.17953.
[39] G. Kresse, J. Furthmüller, Efficient iterative schemes for ab initio total-energy calculations using a plane-wave basis set, Phys. Rev. B 54 (1996) 11169–11186. doi:10.1103/PhysRevB.54.11169.
[40] A. Comas-Vives, Amorphous SiO2 surface models: energetics of the dehydroxylation process, strain, ab initio atomistic thermodynamics and IR spectroscopic signatures, Phys. Chem. Chem. Phys. 18 (2016) 7475–7482. doi:10.1039/C6CP00602G.
[41] S. Gueddida, M. Badawi, S. Lebègue, Grafting of iron on amorphous silica surfaces from ab initio calculations, J. Chem. Phys. 152 (2020) 214706. doi:10.1063/5.0007128.
[42] S. Gueddida, S. Lebègue, M. Badawi, Interaction between transition metals (Co, Ni, and Cu) systems and amorphous silica surfaces: A DFT investigation, Appl. Surf. Sci. 533 (2020) 147422. doi:10.1016/j.apsusc.2020.147422.
[43] S. Gueddida, S. Lebègue, A. Pasc, A. Dufour, M. Badawi, Ab initio investigation of the adsorption of phenolic compounds, co, and h2o over metallic cluster/silica catalysts for hydrodeoxygenation process, Appl. Surf. Sci. 567 (2021) 150790. doi:https://doi.org/10.1016/j.apsusc.2021.150790.